Letter

Earthquakelike dynamics in ultrathin magnetic films

Gianfranco Durin,[1] Vincenzo Maria Schimmenti,[2,3] Marco Baiesi,[4,5] Arianna Casiraghi,[1] Alessandro Magni,[1] Liza Herrera-Diez,[6] Dafiné Ravelosona,[6] Laura Foini,[7] and Alberto Rosso[2]

[1]*Istituto Nazionale di Ricerca Metrologica, Strada delle Cacce 91, 10135 Torino, Italy*
[2]*LPTMS, CNRS, Université Paris-Saclay, Orsay 91405, France*
[3]*Laboratoire Interdisciplinaire des Sciences du Numérique (LISN), TAU team, 91190 Gif-sur-Yvette, France*
[4]*Department of Physics and Astronomy, Università di Padova, Via Marzolo 8, 35131 Padova, Italy*
[5]*INFN, Sezione di Padova, Via Marzolo 8, 35131 Padova, Italy*
[6]*Centre de Nanosciences et de Nanotechnologies, Université Paris-Saclay, CNRS, 91120 Palaiseau, France*
[7]*Institut de Physique Théorique, Université Paris-Saclay, CNRS, 91191 Gif-sur-Yvette, France*

(Received 15 August 2023; revised 6 February 2024; accepted 7 June 2024; published 12 July 2024)

We study the motion of a domain wall on an ultrathin magnetic film using the magneto-optical Kerr effect (MOKE). Our measurements were conducted at magnetic fields approximately 2% of the depinning field where the wall creeps only via thermal activation over the pinning centers present in the sample. Our results show that this creep dynamics is highly intermittent and correlated. A localized instability triggers a cascade, akin to aftershocks following a large earthquake, where the pinned wall undergoes large reorganizations in a compact active region for a few seconds. The analysis of their scale-free statistics enables us to solve an intricate, long-standing problem: thermal avalanches exist in the creep regime and they are depinning-like even for very low magnetic field. Moreover, we show that their sizes and shapes belong to the depinning quenched Kardar-Parisi-Zhang universality class.

DOI: 10.1103/PhysRevB.110.L020405

An important class of future spintronic nanoelectronic devices is based on fully controlling magnetic domain walls in ultrathin films [1,2]. When used as memory devices, for instance, it is fundamental to control their position stability and understand their dynamics under a small perturbation. It is well known that defects naturally present in the nanostructure can pin the domain wall. Consequently, the wall creeps at a finite temperature, with a velocity strongly vanishing with the applied magnetic field. In ultrathin magnetic films, the creep regime holds up to room temperature and well below the depinning field $H_{\rm dep}$. After an initial transient, the wall moves with a small, steady velocity given by the celebrated *creep formula*:

$$\ln v(H) = -\left(\frac{H}{H_0}\right)^{-1/4} + \ln v_0. \tag{1}$$

Here, H_0 and v_0 are materials and temperature-dependent parameters. The exponent $1/4$ is universal and is the true hallmark of creep dynamics. It was first predicted from equilibrium critical exponents in Ref. [3] and identified with the scaling of the Arrhenius activation time over the optimal energy barriers, which grows as $\sim H^{-1/4}$. The reorganization needed to overcome these barriers was found to occur over a typical length scale $L_{\rm opt} \sim H^{-3/4}$ [4–6]. The exponent $1/4$ was measured in Ref. [7] over several decades of velocity and subsequently confirmed in many experiments [8,9]. Despite this success, the nature of creep dynamics remains controversial, with two different scenarios proposed.

The first scenario assumes the presence of a single length scale $L_{\rm opt}$. Below this scale, the dynamics is purely thermal, characterized by an incoherent back-and-forth motion over *equilibrium* barriers. Within this picture, the forward motion of the wall is a sequence of uncorrelated events of length $L_{\rm opt}$ [3].

The second scenario predicts dynamics characterized by two length scales: the forward motion over a size $L_{\rm opt}$ reduces the energy barriers in the nearby region up to a new scale $L_{\rm av}$. Similarly to what is observed in earthquakes, the jump of size $L_{\rm opt}$ acts as the mainshock that produces a cascade of aftershocks of smaller size [10–15]. Hence, the region undergoes a much larger reorganization. Functional renormalization group (FRG) calculations [15] and numerical simulations [6,16–18] showed that this correlated dynamics is controlled by the *depinning* critical exponents. Interestingly, this scenario strongly connects with the thermal facilitation proposed to justify the dynamical heterogeneity in glass-forming liquids [19,20]. The mechanism is similar: the slow relaxation time is dominated by localized slow events that nucleate large responses on a much larger scale. However, experimental evidence of these large reorganizations is still lacking.

In this paper, we report the full dynamical evolution of a domain wall using the magneto-optical Kerr effect (MOKE)

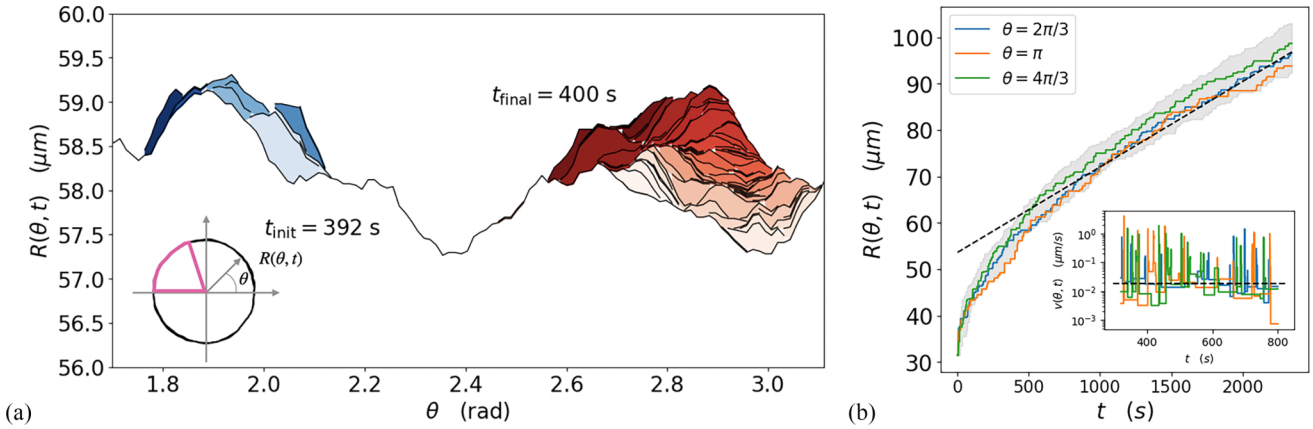

FIG. 1. (a) The evolution of a portion (in pink) of the wall during 8 s. The sequence of the frame events is organized in two distinct clusters (in blue and red). The color gradient represents the progression of time, much faster than the steady velocity $\bar{v}$. (b) Time evolution of wall position $R(\theta, t)$ along three directions (the gray shadow indicates the total spreading). After an initial transient of $t \sim 300$ s, the velocity of the wall decays to its steady value (e.g., $\bar{v} \sim 0.018$ μm/s for $H = 0.14$) [25]. (Inset) Local velocity along three directions. For a given direction θ, we find the times $t_1, t_2, \ldots, t_i \ldots$ where $R(\theta, t)$ changes values. The velocity $v(\theta, t)$ for $t \in [t_i, t_{i+1}]$ is obtained as $(R(\theta, t_{i+1}) - R(\theta, t_i))/(t_{i+1} - t_i)$. The dashed line corresponds to the average steady velocity $\bar{v}$. Each signal displays intermittency with the instantaneous velocity 100 larger than $\bar{v}$.

on an ultrathin magnetic thin film at a magnetic field of 2% the depinning field. As it is clear from the movie in Ref. [21], the dynamics is intermittent and correlated. This reveals the existence of thermal avalanches, never before recorded in experiments. Our analysis demonstrates that the correlations are on scales much larger than L_{opt} and are governed by the depinning critical point, in agreement with the second scenario. Our exponents are in support of the quenched Kardar-Parisi-Zhang (qKPZ) universality class instead of the proposed quenched Edwards-Wilkinson class [6,15–18].

Experimental setting. Field-driven domain wall dynamics is investigated in a Ta(5)/CoFeB(1)/MgO(2)/Ta(3) (thickness in nm) thin film with perpendicular magnetic anisotropy (PMA) [21]. This material is typically very soft, exhibiting a depinning field of 9 mT. The effective DMI can vary from system to system but it is of the order of 0.02–0.08 mJ/m^2, (see Table V in Ref. [22]). In other words, the DW is of Bloch type and no large chiral effects are present. The low density of pinning defects with respect to other PMA systems, such as Co/Pt and Co/Ni multilayers, makes it a good candidate to study domain wall dynamics [23]. The competition between domain wall elasticity and the local disorder results in a thermally activated creep motion for driving fields up to the depinning field [24]. A magnetic bubble domain is initially nucleated with a ∼30 μm radius in the presaturated film through a short field pulse. The subsequent slow expansion occurs under a small continuous perpendicular applied field. Here we use $H = 0.13,\ 0.14,\ 0.15,\ 0.16$ mT, corresponding to $< 2\,\%$ of H_{dep}. This ultraslow creep dynamics is captured through MOKE microscopy. MOKE images with a spatial resolution of 400 nm are acquired every 200 ms until the bubble radius has increased to about 100 μm. Even at the lowest applied field, the bubble domain conserves its circular shape and boundary smoothness upon expansion, indicating weak random pinning. The limitations in the spatial resolution and in the acquisition rate do not allow us to detect the fast dynamics of the domain wall at the nanoscale, but we can resolve the motion of the wall by estimating the time at which each pixel changes its gray level (see Sec. I of Ref. [21] for a detailed description of the procedure). Remarkably, the set of switched pixels between two consecutive images is always connected in space, and we define it as a single *frame event*.

Analysis of experimental spatiotemporal patterns. The dynamics of the domain observed frame by frame displays two important features:

(1) The bubble always expands and never comes back. As shown in Fig. 1(b), the position of the interface $R(\theta, t)$ along any direction is a nondecreasing function of time. Moreover, after an initial transient, the velocity of the wall decays to its steady value $\bar{v}$. However, the local velocity (inset) displays strong intermittency in time.

(2) The motion presents spatial correlations well above the pixel size. Indeed, Fig. 1(a) shows that each event frame corresponds to a compact spatial region, and events of subsequent frames tend to cluster in space. See the movie in Ref. [21] to visualize the full dynamics of the bubble. Similar to earthquakes, a first main event seems to trigger a cascade of aftershocks.

These two features support the second scenario for which the initial reorganization of a region of size L_{opt} is followed by a cascade of frame events on much larger scales. Indeed, the simple thermal activation is characterized by incoherent back-and-forth motion representing the attempts to overcome the energy barrier. Here, instead, we observe a coherent forward motion on timescales much faster than the steady velocity. This conclusion is also coherent with the estimation of L_{opt} given in Refs. [8,15]:

$$L_{opt} \sim L_C (H_{dep}/H)^{3/4} \tag{2}$$

with L_C the microscopic Larkin length at which the wall fluctuations become of the order of its thickness. In the materials used in this work, the Larkin length is approximately $L_C \sim 100$ nm. Hence, L_{opt} is ∼380–400 nm. This scale is just

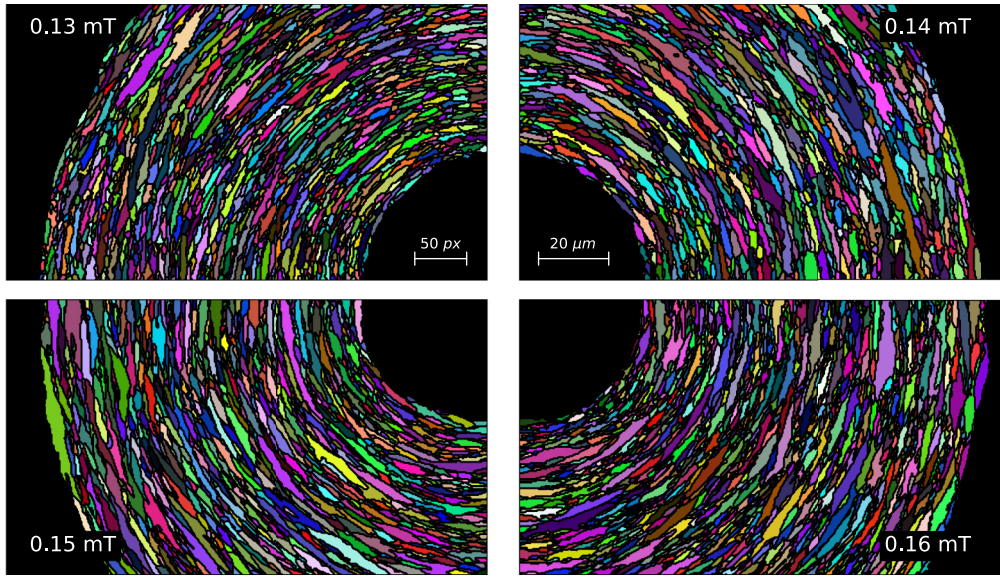

FIG. 2. Sequences of clusters at different applied fields, which start from the initial bubble (the central black sector at the inner corner of the images) and grow until the radius is about 100 μm. See also the movie in Ref. [21].

below the single pixel size of 400 nm and is too small to be experimentally accessible. To quantify the spatial correlations observed beyond L_{opt}, we construct clusters of frame events close in space and time via a simple algorithm that depends on two parameters Δt and Δs. This method is simpler than the clustering method used for earthquakes [10] because elasticity is short-ranged for a magnetic domain wall. Hence, its aftershocks occur in a compact region. On the contrary, the elasticity is long-ranged in the Earth's crust, and identifying earthquake clusters is more subtle. In practice, we start from an initial frame event (the epicenter of the cluster) and include all frame events within a time window Δt and a distance Δs. Section III of Ref. [21] shows that our analysis is robust upon variations of Δt and Δs. Figure 2 shows the clusters obtained using this procedure. Each cluster can be characterized by two quantities, namely, the size S (the colored areas in Fig. 2) and the longitudinal length ℓ (see Sec. IV of Ref. [21]). Both quantities display scale-free statistics [Figs. 3(a) and 3(b)], with exponents which are incompatible with the equilibrium exponents used to characterize the barrier of the energy landscape up to the scale L_{opt}. It is thus tempting to interpret these clusters as avalanches at the depinning transition as suggested by the numerical simulations on directed interfaces in Ref. [17]. In those simulations, however, avalanches are very

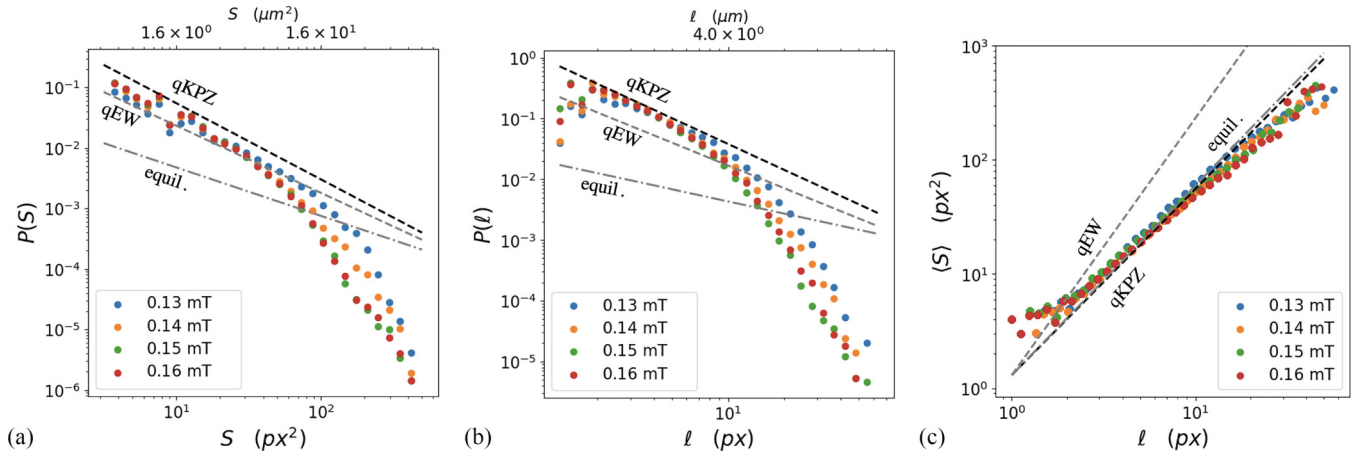

FIG. 3. (a) Cluster size S and (b) longitudinal length ℓ distributions for different magnetic fields. (c) Cluster size versus their longitudinal length. The clusters have been obtained for $\Delta t = 8$ frames and $\Delta s = 2$ pixels. The first two panels are compatible with qEW and qKPZ universality classes but not with the equilibrium exponents (see Table I for their values). The value of the roughness exponents from (c) is computed using the power law scaling $S \sim \ell^{1+\zeta}$. The measured value is compatible with both $\zeta_{\text{qKPZ}} = 0.63$ and $\zeta_{\text{equilibrium}} = 2/3$, but exclude the qEW universality class $\zeta_{\text{qEW}} = 1.25$. Combining these findings leaves the qKPZ universality class as the sole possible candidate for describing the creep motion in our experiment.

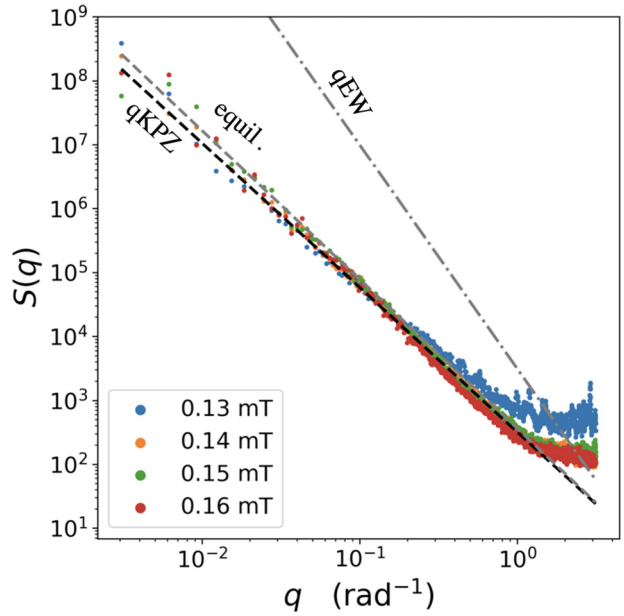

FIG. 4. Structure factor $S(q)$ computed by averaging over time the Fourier transform $\rho(q,t)$ of $\rho(\theta,t) = R(\theta,t) - \overline{R}(t)$, i.e., $S(q) = \langle \rho(q,t)\rho(-q,t)\rangle_t$. Using the power law scaling an $S(q) \sim q^{-(1+2\zeta)}$ at small q, we compute a value of the roughness exponent in perfect agreement with the one obtained in Fig. 3(c).

fat in the growth direction (i.e., the direction of propagation of the interface) consistently with the quenched Edwards Wilkinson (qEW) depinning. Here clusters are instead elongated objects as shown in Figs. 2 and 3(c) where $S \sim \ell^{1+\zeta}$ results in a roughness exponent $\zeta \sim 0.63$. This exponent excludes the possibility of qEW depinning but is consistent with the qKPZ depinning. We corroborate this conclusion with an independent study of the roughness of the whole interface. Following the method proposed in Ref. [26], we compute the structure factor $S(q)$ that, as discussed in Ref. [17], displays a $q^{-(1+2\zeta)}$ dependence at small values of the wave number q. Figure 4 shows that the interface's roughness exponent ζ is consistent with the one characterizing the elongated shape of the cluster. Our results thus prove that the spatial correlations observed beyond the scale L_{opt} are in the qKPZ depinning. The qKPZ universality class reveals the presence of anisotropic disorder in our experiment. This feature was not included in previous numerical simulations.

Conclusions. The celebrated creep formula (1) rests on the hypothesis that the key feature determining a wall motion is optimized excitations of size L_{opt}. Our work focuses on intermittently occurring rapid movements along a magnetic wall and unveils their spatial organization, extending on scales much more extensive than L_{opt}. These patterns are reminiscent of the sequences of main shock and aftershocks in earthquakes, even if the two have important differences. The size and the shape of the patterns studied here display the same statistics of the avalanches recorded at the depinning magnetic field but with a much slower evolution.

A previous experimental study [27] highlighted the existence of a weakly correlated motion. Their analysis supports a depinning dynamics in the qEW universality class. Still,

TABLE I. Theoretical values of critical exponents for depinning (qEW and qKPZ universality classes) and equilibrium: the roughness exponent ζ [$S \sim \ell^{1+\zeta}$, and $S(q) \sim q^{1+2\zeta}$], the exponent τ of cluster size distribution $P(S) \sim S^{-\tau}$, and the exponent κ for longitudinal length distribution $P(\ell) \sim \ell^{-\kappa}$.

	ζ	τ	$1+2\zeta$	κ
Equilibrium	2/3	4/5	7/3	2/3
qEW	1.25	1.11	3.50	1.25
qKPZ	0.63	1.26	2.27	1.42

the authors of Ref. [27] observe that this conclusion is incompatible with the roughness exponent $\zeta = 0.69 \pm 0.07$ accurately measured in Ref. [7]. Our results solve this intricate puzzle and show solidly that the depinning qKPZ universality class correctly describes both the roughness and the statistics of thermal avalanches at large scales. However, the emergence of KPZ dynamics at depinning must be sustained by anisotropy in the material, and its origin calls for further understanding.

The scenario emerging from our results should be tested in other examples of elastic disordered systems such as ferroelectric domain walls [28–30] or crack propagation [31]. Interestingly, a similar scenario was recently reported for a different class of disordered systems, such as amorphous solids or glass-forming liquids. Simulations on elastoplastic models have shown how localized excitations can trigger cascades of faster events [19,20]. Hence, thermally facilitated avalanches can be pretty generic in disordered systems. They reveal the complex nature of disordered energy landscapes that cannot be described simply by a sequence of uncorrelated elementary excitations.

The results reported here can also have significant consequences in the field of spintronics. The creep dynamics of a bubble domain is, in fact, at the base of one of the most used methods to determine the interfacial Dzyaloshinskii-Moriya interaction (DMI). This is a chiral interaction responsible for the occurrence of topological spin structures, such as chiral domain walls and skyrmions, considered the most promising information carriers in future spintronics technologies [22]. The determination of the DMI constant is based on the asymmetric expansion of the bubble under an in-plane magnetic field, with the domain wall velocity measured by dividing the displacement between two MOKE snapshots over their time interval. Figure 1(b) actually suggests that the velocity is constant only at large times/displacements, and thus that this procedure could be misleading. In addition, theoretical expressions to evaluate the DMI field from the velocity curve are primarily phenomenological, and a more accurate description of the domain wall dynamics, such as the qKPZ reported here, could highly improve the fits of the data. We hope these considerations shed some light on a more accurate determination of DMI value and solve the contradictions with other popular methods, such as the Brillouin light scattering.

Acknowledgements. V.M.S. acknowledges 80Prime CNRS support for the project CorrQuake. M.B. is supported by the University of Padova, Research Grant No. BAIE_BIRD2021_01.

[1] S. Parkin and S.-H. Yang, Memory on the racetrack, Nat. Nanotechnol. **10**, 195 (2015).

[2] K. Gu, Y. Guan, B. K. Hazra, H. Deniz, A. Migliorini, W. Zhang, and S. S. P. Parkin, Three-dimensional racetrack memory devices designed from freestanding magnetic heterostructures, Nat. Nanotechnol. **17**, 1065 (2022).

[3] L. B. Ioffe and V. M. Vinokur, Dynamics of interfaces and dislocations in disordered media, J. Phys. C: Solid State Phys. **20**, 6149 (1987).

[4] M. Dong, M. C. Marchetti, A. A. Middleton, and V. Vinokur, Elastic string in a random potential, Phys. Rev. Lett. **70**, 662 (1993).

[5] E. Agoritsas, V. Lecomte, and T. Giamarchi, Disordered elastic systems and one-dimensional interfaces, Phys. B: Condens. Matter **407**, 1725 (2012), Proceedings of the International Workshop on Electronic Crystals (ECRYS-2011).

[6] E. E. Ferrero, L. Foini, T. Giamarchi, A. B. Kolton, and A. Rosso, Creep motion of elastic interfaces driven in a disordered landscape, Annu. Rev. Condens. Matter Phys. **12**, 111 (2021).

[7] S. Lemerle, J. Ferré, C. Chappert, V. Mathet, T. Giamarchi, and P. Le Doussal, Domain wall creep in an Ising ultrathin magnetic film, Phys. Rev. Lett. **80**, 849 (1998).

[8] K.-J. Kim, J.-C. Lee, S.-M. Ahn, K.-S. Lee, C.-W. Lee, Y. J. Cho, S. Seo, K.-H. Shin, S.-B. Choe, and H.-W. Lee, Interdimensional universality of dynamic interfaces, Nature (London) **458**, 740 (2009).

[9] V. Jeudy, A. Mougin, S. Bustingorry, W. Savero Torres, J. Gorchon, A. B. Kolton, A. Lemaître, and J.-P. Jamet, Universal pinning energy barrier for driven domain walls in thin ferromagnetic films, Phys. Rev. Lett. **117**, 057201 (2016).

[10] M. Baiesi and M. Paczuski, Scale-free networks of earthquakes and aftershocks, Phys. Rev. E **69**, 066106 (2004).

[11] E. A. Jagla and A. B. Kolton, A mechanism for spatial and temporal earthquake clustering, J. Geophys. Res. **115**, B05312 (2010).

[12] E. A. Jagla, F. P. Landes, and A. Rosso, Viscoelastic effects in avalanche dynamics: A key to earthquake statistics, Phys. Rev. Lett. **112**, 174301 (2014).

[13] C. H. Scholz, *The Mechanics of Earthquakes and Faulting*, 3rd ed. (Cambridge University Press, Cambridge, 2019).

[14] V. Repain, M. Bauer, J.-P. Jamet, J. Ferré, A. Mougin, C. Chappert, and H. Bernas, Creep motion of a magnetic wall: Avalanche size divergence, EPL **68**, 460 (2004).

[15] P. Chauve, T. Giamarchi, and P. Le Doussal, Creep and depinning in disordered media, Phys. Rev. B **62**, 6241 (2000).

[16] A. B. Kolton, A. Rosso, T. Giamarchi, and W. Krauth, Creep dynamics of elastic manifolds via exact transition pathways, Phys. Rev. B **79**, 184207 (2009).

[17] E. E. Ferrero, L. Foini, T. Giamarchi, A. B. Kolton, and A. Rosso, Spatiotemporal patterns in ultraslow domain wall creep dynamics, Phys. Rev. Lett. **118**, 147208 (2017).

[18] V. H. Purrello, J. L. Iguain, A. B. Kolton, and E. A. Jagla, Creep and thermal rounding close to the elastic depinning threshold, Phys. Rev. E **96**, 022112 (2017).

[19] M. Ozawa and G. Biroli, Elasticity, facilitation, and dynamic heterogeneity in glass-forming liquids, Phys. Rev. Lett. **130**, 138201 (2023).

[20] A. Tahaei, G. Biroli, M. Ozawa, M. Popović, and M. Wyart, Scaling description of dynamical heterogeneity and avalanches of relaxation in glass-forming liquids, Phys. Rev. X **13**, 031034 (2023).

[21] See Supplemental Material at http://link.aps.org/supplemental/10.1103/PhysRevB.110.L020405 for (S1) Sample preparation and experimental details (S2) Resolving the wall dynamics (S3) Clustering algorithm (S4) Longitudinal length of the cluster (S5) Movie of the experiment at $H = 0.13$ mT.

[22] M. Kuepferling, A. Casiraghi, G. Soares, G. Durin, F. Garcia-Sanchez, L. Chen, C. H. Back, C. H. Marrows, S. Tacchi, and G. Carlotti, Measuring interfacial Dzyaloshinskii-Moriya interaction in ultrathin magnetic films, Rev. Mod. Phys. **95**, 015003 (2023).

[23] C. Burrowes, N. Vernier, J.-P. Adam, L. Herrera Diez, K. Garcia, I. Barisic, G. Agnus, S. Eimer, J.-V. Kim, T. Devolder *et al.*, Low depinning fields in Ta-CoFeB-MgO ultrathin films with perpendicular magnetic anisotropy, Appl. Phys. Lett. **103**, 182401 (2013).

[24] L. Herrera Diez, F. García-Sánchez, J.-P. Adam, T. Devolder, S. Eimer, M. S. El Hadri, A. Lamperti, R. Mantovan, B. Ocker, and D. Ravelosona, Controlling magnetic domain wall motion in the creep regime in He^+-irradiated CoFeB/MgO films with perpendicular anisotropy, Appl. Phys. Lett. **107**, 032401 (2015).

[25] An increase in steady velocity was observed during the expansion of small magnetic bubbles for magnetic fields close to the depinning threshold [32]. However, for the very small fields used in our study, the transient period is much longer and dominates the dynamics.

[26] K. A. Takeuchi and M. Sano, Universal fluctuations of growing interfaces: Evidence in turbulent liquid crystals, Phys. Rev. Lett. **104**, 230601 (2010).

[27] M. P. Grassi, A. B. Kolton, V. Jeudy, A. Mougin, S. Bustingorry, and J. Curiale, Intermittent collective dynamics of domain walls in the creep regime, Phys. Rev. B **98**, 224201 (2018).

[28] T. Tybell, P. Paruch, T. Giamarchi, and J.-M. Triscone, Domain wall creep in epitaxial ferroelectric $Pb(Zr_{0.2}Ti_{0.8})O_3$ thin films, Phys. Rev. Lett. **89**, 097601 (2002).

[29] B. Casals, G. F. Nataf, and E. K. Salje, Avalanche criticality during ferroelectric/ferroelastic switching, Nat. Commun. **12**, 345 (2021).

[30] P. Tückmantel, I. Gaponenko, N. Caballero, J. C. Agar, L. W. Martin, T. Giamarchi, and P. Paruch, Local probe comparison of ferroelectric switching event statistics in the creep and depinning regimes in $Pb(Zr_{0.2}Ti_{0.8})O_3$ thin films, Phys. Rev. Lett. **126**, 117601 (2021).

[31] L. Ponson, D. Bonamy, and E. Bouchaud, Two-dimensional scaling properties of experimental fracture surfaces, Phys. Rev. Lett. **96**, 035506 (2006).

[32] K.-W. Moon, J.-C. Lee, S.-G. Je, K.-S. Lee, K.-H. Shin, and S.-B. Choe, Long-range domain wall tension in Pt/Co/Pt films with perpendicular magnetic anisotropy, Appl. Phys. Express **4**, 043004 (2011).